Journal of Magnetics 3(4), 127-133 (1998)

Spin Dependent Transport Phenomena for Annealed $Co_{46}Al_{19}O_{35}$ Granular Thin Films

Jae-Geun Ha

Dept. of Electronic Materials Engineering, Kwangwoon University, 447-1 Wolgye-dong, Nowon-ku, Seoul 139-701, Korea

(Received 11 November 1998)

I have overviewed the change in GMR on annealing, in conjunction with the change in microstructure. The $Co_{46}Al_{19}O_{35}$ granular thin films were annealed at 300°C for various annealing time to change the microstructure. The magnitude of GMR decreases considerably with increasing annealing time, although the size of Co granules estimated from TEM observation show a small change. Parameter fits of magnetization curves and magnetoresistance curves to the Langevin function suggest that large clusters consisting of several small Co granules, which are coupled ferromagnetically, are related with the decrease of GMR on annealing. The temperature dependence of electrical resistivity (ρ) shows the relationship of log ρ versus $T^{-1/2}$ for the sample annealed for 10 min., 1 hr. and 6 hrs. However, the sample annealed for 38 hrs. shows the relationship of log ρ versus $T^{1/4}$, which represents a significant change in the transport mechanism.

1. Introduction

Spin-dependent transport phenomena in artificial nanostructures have attracted much attention from fundamental and practical points of view. Since giant magnetoresistance (GMR) was discovered in Fe/Cr multilayers [1], the GMR phenomena have been investigated intensively in various metallic multilayers, sandwich films and granular alloys [2]. The origin for GMR in these metallic systems is spin dependent scattering of conduction electrons [3, 4]. The constituent phases in these are all metallic; therefore, the electrical resistivities of the materials which show GMR are low in general. If electrical resistivity increases, the effect of spin dependent scattering, i.e. GMR, is expected to smear out, because the factor of spin dependent scattering increases by shortened electron mean free path and spin diffusion length. However, Fujimori et al. found that sputtered Co-Al-O granular thin films exhibit as much as 8% of GMR under an applied magnetic field of 12 kOe at room temperature, in spite of the fact that the electrical resistivity of these films is very high [5, 6]. Mitani *et al.* reported that the GMR mechanism found in Co-Al-O was obviously attributed to the spin-dependent tunneling [6].

The physical phenomena of spin dependent tunneling has also has been discussed in a sandwich-type junction composed of ferromagnetic metal/insulator/ferromagnetic metal [7-9]. The same situation is considered in a superparamagnetic metal-insulator granular system, because the system is thought to be an assembly of many small ferromagnetic metal/insulator/ferromagnetic metal junctions. The magnetic moments of Co granules are randomly oriented at zero magnetic field because of the superparamagnetic state, however they are aligned to one direction when external magnetic field is applied. Consequently the resistivity decreases as a function of applied field, because the probability of electron tunneling increases by the application of magnetic field. However, the detailed behavior and mechanism of the GMR has not been fully elucidated yet. It is important to understand the relationship between the GMR behavior and microstructures. In this paper, we have investigated the change in GMR on annealing, in conjunction with the change in microstructure investigated from TEM observation and the analysis of superparamagnetic behavior. And, we have investigated systematically the transport and GMR behavior on annealing including the case annealed for elongated time, 38 hours.

2. Experimental Procedure

The Co-Al-O granular thin films were prepared on glass substrates by a reactive sputtering method using a $Co_{72}Al_{28}$ alloy target. The sputtering gas used was a mixed $Ar+O_2$. The details on the sample preparation were described elsewhere [5, 6]. Samples were annealed in vacuum-sealed glass tubes at 300 °C for 10 min., 1 hr., 6 hrs., and 38 hrs. The magnetization curve was measured using a SQUID magnetometer (QUANTUM DESIGN, MPMS) with the field applied up to 50 kOe. The magnetoresistance (MR) was measured at room temperature, 77 K, and 4.2 K under the applied field of about 7 kOe by a conventional four-

probe method. The magnitude of GMR is defined as $\Delta\rho/\rho_{max}$, where $\Delta\rho$ is ρ-ρ_{max}, ρ_{max} is the maximum resistivity, respectively. In order to evaluate the microstructures quantitatively, small angle X-ray scattering (SAXS) has been measured by using a conventional X-ray generator with a Mo target. Transmission electron microscopy (TEM) and high resolution transmission electron microscopy (HRTEM) observations have also been made using Philips CM-200 and JEOL-4000EX electron microscopes, respectively. The chemical composition was analyzed by Rutherford backscattering spectroscopy (RBS). The composition of the Co-Al-O granular film is $Co_{46}Al_{19}O_{35}$. The present investigation has been performed on this series.

3. Results and Discussions

3.1 Electrical resisitivity and microstructures

The temperature dependence of the electrical resistivity ρ for as-deposited and annealed samples is shown in Fig. 1(a). It shows the good linear relationship of log ρ versus $T^{-1/2}$ for both as-deposited and all the annealed samples as seen in Fig. 1(b).

The relation of log ρ versus $T^{1/2}$ was first derived by Sheng *et al.* by taking into account the tunneling and thermal activation process for electrical transport in insulating granular systems [10, 11]. In insulating granular systems, conduction electrons can flow weakly by tunneling between metallic granules. This tunneling probability is proportional to $\exp\{-2(2\pi/h)\ (2m\phi)^{1/2}\ s\}$, where h is the Plank constant, m the effective electron mass, ϕ the effective barrier height, and s the barrier width. In case of insulating granular systems, we must take into account the breakdown of charge neutrality in the metallic granules associated with tunneling. Sheng *et al.* considered a model that the electrons thermally activated by this increase in the Coulomb energy can tunnel. The probability associated with this process is proportional to $\exp\{E_c/2k_BT\}$, where E_c is the Coulomb energy increased for a granule, k_B the Boltzman constant, T the absolute temperature. Sheng *et al.* calculated the electrical resistivity by taking into account these two probabilities and obtained the formula expressed as

$$\rho = \rho_o \exp\{2(C/k_B)^{1/2}T^{-1/2}\} \tag{1}$$

where C is the tunneling activation energy, and given by

$$C = \chi S E_c \tag{2}$$

where $\chi = 2\pi/h\sqrt{2m\phi}$, S is the average intergranular distance.

Eq. (1) can be transformed to

$$\log \rho = 2(C/k_B)^{1/2}T^{-1/2} + const. \tag{3}$$

The good linear relationship of log ρ versus $T^{-1/2}$ in Fig. 1(b) shows the tunneling transport for both as-deposited and all the annealed samples.

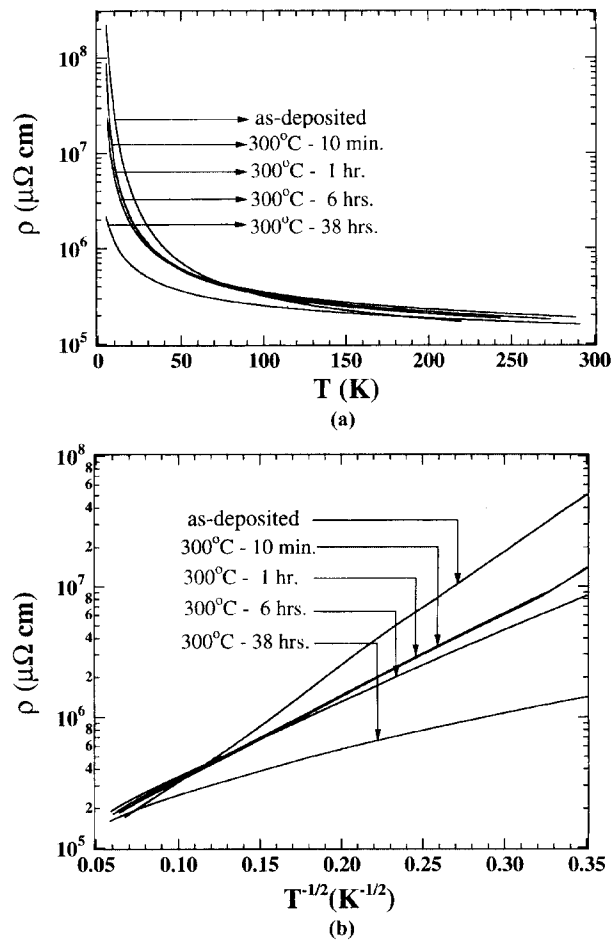

Fig. 1. Temperature dependence of electrical resistivity (ρ) for as-deposited and annealed $Co_{46}Al_{19}O_{35}$ granular thin films; (a) log ρ vs. T, (b) log ρr vs. $T^{-1/2}$.

C can be rewritten as [11]

$$C = \frac{2\chi e^2}{\varepsilon} \cdot \frac{(S/d)^2}{(1/2+S/d)} \tag{4}$$

where d is the average size of granules, e is the electron charge and ε is the dielectric constant of Al_2O_3. Equation (4) indicates that C is constant in case S/d is constant.

C is shown as a function of annealing time in Fig. 2. C is estimated to be 89 meV for the as-deposited sample. With increasing annealing time, C decreases gradually to 35 meV. If Co granules grow by coarsening process with increasing annealing time, local composition should not change, and S/d, and therefore, C should be constant. The change of C on annealing indicates that Co granules do not grow simply.

In order to evaluate the change in microstructures on annealing, we made the structural analyses by using TEM, HRTEM and SAXS. Fig. 3 shows HRTEM images for the as-deposited and annealed samples. The microstructures of the samples are composed of fine granules. These granules

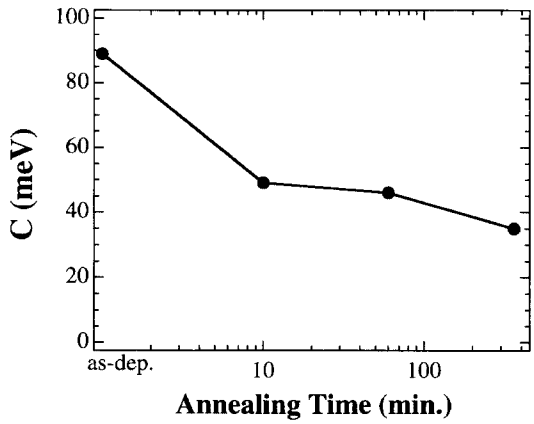

Fig. 2. Tunneling activation energy (C) for a $Co_{46}Al_{19}O_{35}$ granular thin film as a function of annealing time.

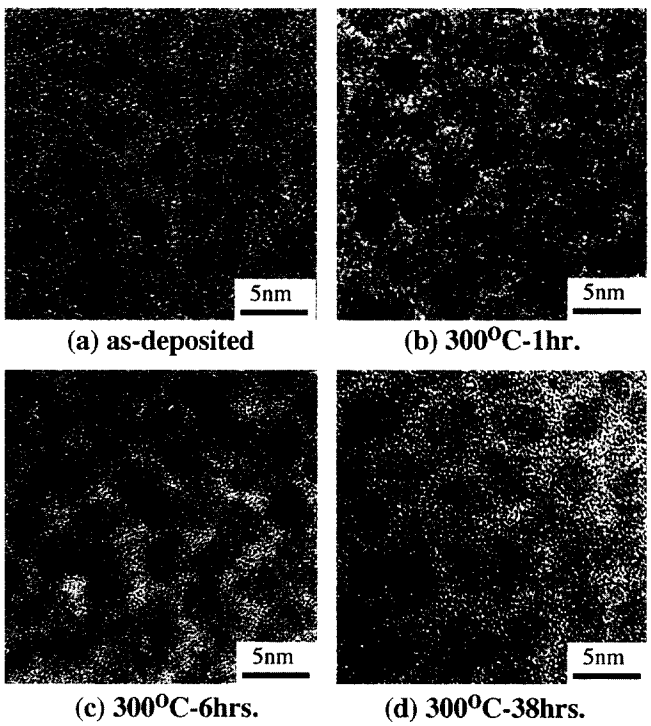

Fig. 3. HRTEM micrographs of $Co_{46}Al_{19}O_{35}$ granular thin films: (a) as-deposited, (b) annealed at 300°C for 1 hour, (c) annealed at 300°C for 6 hours, (d) annealed at 300°C for 38 hours.

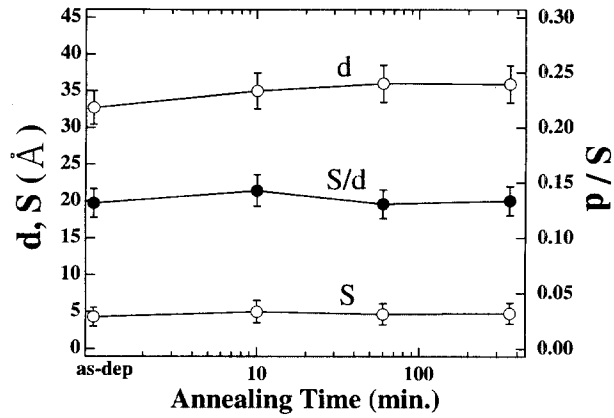

Fig. 4. Average intergranule distance (S) estimated by SAXS and average granule diameter (d) evaluated from TEM micrographs for a $Co_{46}Al_{19}O_{35}$ granular film as a function of annealing time.

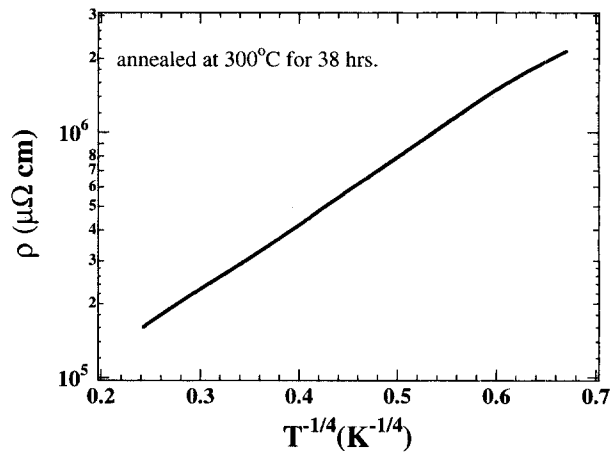

Fig. 5. Temperature dependence of the electrical resistivity (ρ) for the $Co_{46}Al_{19}O_{35}$ granular thin film, annealed at 300°C for 38 hours. log ρ is plotted as a function of $T^{-1/4}$.

are surrounded by brightly imaging channels. It is considered that the concentration of oxygen in the brightly imaging regions is higher than in the granules, because higher concentration of light elements makes the phase more transparent to electron [12]. The brightly imaging channels are perfectly continuous, and the granules appear to be isolated. A remarkable feature is that the granule size for the as-deposited sample is almost the same as that for the annealed samples. The average granule sizes for both as-deposited and annealed samples are approximately 30~40Å diameters. The average intergranular distance (S) estimated by SAXS and average granule diameter (d) evaluated from TEM micrographs are shown as a function of annealing time in Fig. 4. We find that *S/d* is constant irrespective of annealing time, because *d* and *S* increase simultaneously. Then, one question arises: why does *C* decrease with increasing annealing time? One possible explanation for the decrease in *C* is the formation of large Co clusters constituting of several small Co granules, which are coupled electrically and magnetically. We will make the detailed discussions about this assumption in section 3.2.

Another remarkable feature in Fig. 1(b) is that the sample annealed for 38 hours does not satisfy the linear relationship of log ρ versus $T^{-1/2}$. The plot of log ρ versus $T^{-1/4}$ is shown in Fig. 5, compared to that of log ρ versus $T^{-1/2}$. The relationship of log ρ versus $T^{-1/4}$ represents the variable range hopping transport in amorphous semiconductors. Hopping conduction is a term coined to denote the electrical conduction process which is the result of two combined mechanisms: thermal activation and tunneling. Mott was the first one to show that two nominally independent processes can actually couple to result in non-activation type of behavior [13]. The microstructure such as the size of Co granules estimated by TEM and HRTEM

for the sample annealed for 38 hours did not change significantly as shown in Fig. 3. This suggests that the change in transport mechanism on annealing is not mainly due to the change of the granule size. The origin for the transition from log $\rho \propto T^{-1/2}$ to log $\rho \propto T^{-1/4}$ is not clear at present.

3.2 Superparamagnetic analysis of magnetization curve

We analyze the magnetization behavior by making parameter fits to magnetization curves to the Langevin function. The magnetization of superparamagnetic particles can be described by the Langevin function [14], assuming all particles have the same magnetization

$$\frac{M(T,H)}{M_S} = L(a) = cotha - \frac{1}{a}$$
$$M(T,H) = M_S L(a) \tag{5}$$

where the parameter a is the ratio between magnetic energy of one particle and its thermal energy. This gives a direct access to the magnetic moment of one particle, from which its volume can be estimated via the magnetization of the ferromagnetic phase,

$$a = \frac{\mu H}{k_B T} \tag{6}$$

T is the temperature, and k_B is the Boltzman constant. Equation (5) was fitted to experimental data for both as-deposited and annealed samples. If we consider the granule size, which is estimated by TEM, we found a strong deviation from the theoretical data calculated from Eq. (5). Obviously, the simplifications are too rough, so we take into account that there is not only one size of Co granule, but a appropriate size distribution. If we consider a size distribution, Eq. (5) can be rewritten by

$$M_{total}(T,) = M_S \sum_i x_i L(a_i) \; (\sum_i x_i = 1) \tag{7}$$

where subscript i denote the size of granule and x_i is the normalized granule density. Calculations using the size distribution functions such as a rectangular distribution, a Gaussian distribution were performed but also did not fit the experimental data. A good agreement with the experimental data was found in case of considering a log normal size distribution (LNDF), as it has been found for fine metal particles produced by inert-gas evaporation [15]. A LNDF f_r with standard deviation s and the mean radius r_m is given like this:

$$f_r = \frac{1}{\sqrt{2}\sigma_m^2} \exp\left(\frac{\ln^2(r/r_m)}{2\sigma_m^2}\right) \tag{8}$$

A fitting results were obtained with LNDF's, as shown in the upper figures of Fig. 6. The calculated values which were obtained by using eqs. (7) and (8) are shown by the solid line in the upper figures of Fig. 6. The size distribution function was approximately by a step function as shown in the lower figures of Fig. 6. The agreement with the experimental data points is remarkably good. We found that LNDF's of all the annealed samples are different from

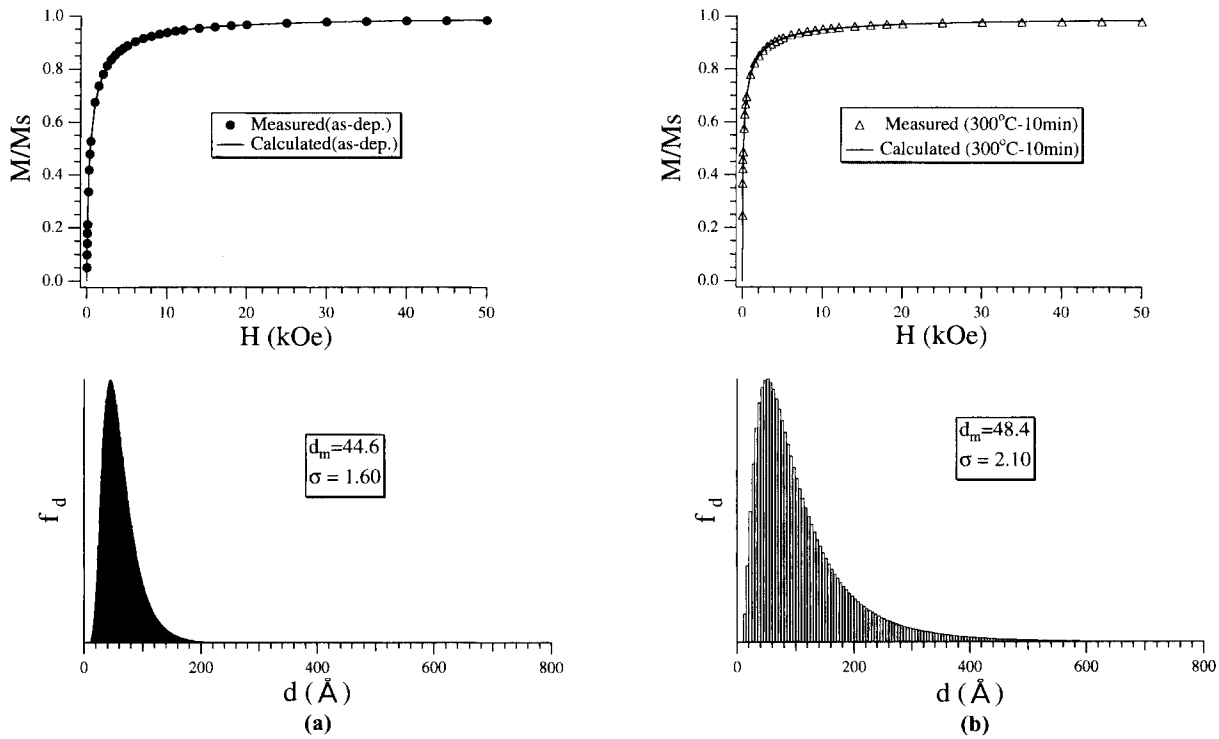

Fig. 6. Magnetization curves for the (a) as-deposited (b) annealed at 300°C for 10 min. (c) annealed at 300°C for 1 hr. (d) annealed at 300°C for 6 hr. The solid line of the upper figure represents the calculated curves assuming LNDF such as the lower figure.

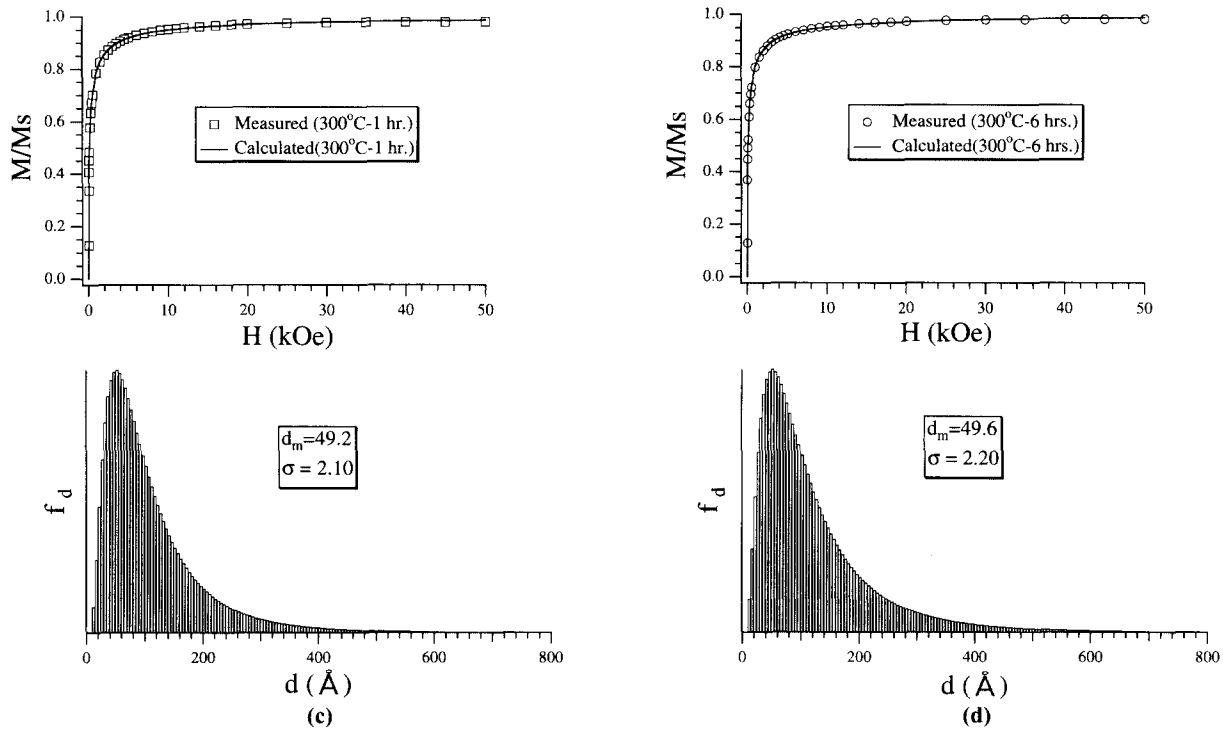

Fig. 6. Continued.

that of as-deposited sample. The width of the LNDF's are broader, and are extended to larger Co granules compared to as-deposited sample.

However, the size of Co granules estimated by TEM observation did not change significantly. The Co granule sizes of all the annealed samples are found to be approximately 10% increase compared with as-deposited sample as shown in Fig. 4. The granule size estimated by TEM, d_{TEM} and the average granule size inferred by parameter fit of magnetization curve, d_{mag} are shown in Table 1. In the case of 38-hrs. annealed sample, we can not obtain d_{mag} by parameter fit of magnetization curve. This suggests that the microstructure of 38-hrs. annealed sample is different from that of other annealed samples.

The differences of d_{TEM} and d_{mag} are large, even though in case of as-deposited sample. Then what is the physical origin of the difference with the d_{TEM} and d_{mag}? We think that d_{mag} can be explained as the size of large cluster consisting of small Co granules, which are coupled ferromagnetically. With increasing annealing time, the d_{mag} increases smoothly. The d_{mag} increases with increasing annealing time, because the intergranular distance become smaller with increasing annealing time and result in the formation of larger clusters. This suggests that several Co granules are coupled ferromagnetically to form a large magnetic cluster which might behave as a magnetic unit.

Table 1. The granule size estimated by TEM, d_{TEM} and the average granule size inferred by parameter fit of magnetization curve, d_{mag} for $Co_{46}Al_{19}O_{35}$ granular thin films

Sample	d_{TEM} (Å)	d_{mag} (Å)	σ	d_m (Å)
as-deposited	33±1	62	1.6	44.6
300°C-10 min.	35±1	112	2.1	48.4
300°C-60 min.	36±1	113	2.1	49.2
300°C-360 min.	35±1	126	2.2	49.6

Parameter fits of magnetization curves to the Langevin function suggest the existence of large cluster consisting of small granules which are coupled ferromagnetically. But such large clusters are not observed by TEM, even though by HRTEM. If large cluster consist of small granules which are not physically but only magnetically, we can not observe such a large cluster. Then, one question can be arised? What is the origin of large cluster i.e. d_{mag}? We think that this is related with the concept of the resistance quantum. If the tunnel resistance between granules in insulating granular system is below the resistance quantum which is about 20 kΩ, the conduction between granules is to be metallic [16]. In insulating granular system, the average intergranular distance in the compositions showing the GMR phenomena is about 4~10Å [12]. Therefore, it is reasonable that there are several Co granules whose tunnel resistance are below the quantum resistance, because of the size distribution such as LNDF in granular system. These phenomena can appear in case the Co concentration is high. Therefore, the above discussion can be realized in this system, because the composition of the present investigation, $Co_{46}Al_{19}O_{35}$ is high. Recently, we found the existence of the critical composition, which showing the difference between d_{TEM} and d_{mag} by parameter fit of magnetization curve in other compositions. The details are published elsewhere. Figure 7 shows the schematic illustration of model representing the formation of clusters consisting of

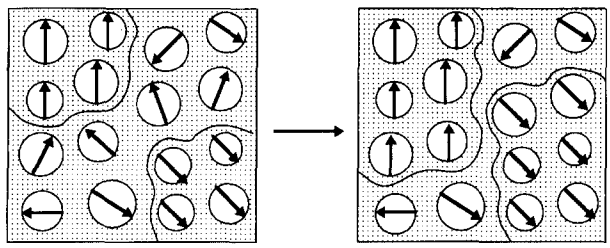

Fig. 7. Schematic illustration of model explaining the experimental results: (a) as-deposited, (b) after annealing.

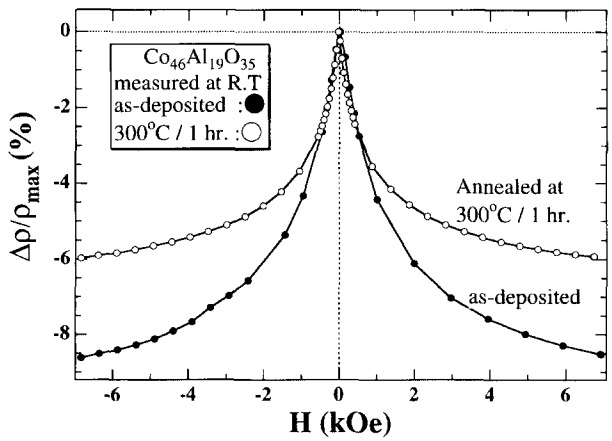

Fig. 8. Magnetoresistance curves for the as-deposited and 300°C-1 hour annealed $Co_{46}Al_{19}O_{35}$ granular thin film.

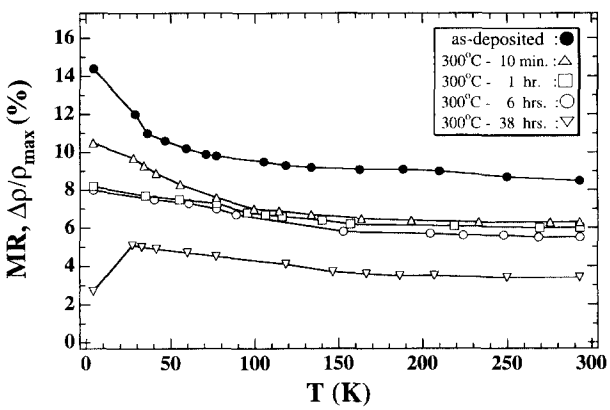

Fig. 9. Temperature dependence of GMR for as-deposited and annealed $Co_{46}Al_{19}O_{35}$ granular thin film.

several small Co granules, which are coupled ferromagnetically. With increasing annealing time, the size of cluster increases compared to that of as-deposited.

3.3 Giant Magnetoresistance (GMR)

Figure 8 shows magnetoresistance ratio ($\Delta\rho/\rho_{max}$) curve for the (a) as-deposited (b) annealed at 300°C for 1 hour. Magnetoresistance ratio for the annealed sample decreases compared with that for the as-deposited sample. Figure 9 shows the temperature dependence of magnetoresistance ratio for as-deposited and annealed samples. The magnitude of GMR decreases considerably with increasing annealing time. Particularly, GMR reveals a noticeable decrease at low temperatures on annealing. The change in microstructure i.e. the formation of ferromagnetically coupled cluster seems to be closely related with the decrease of the GMR on annealing.

Although the transport mechanism was changed to hopping transport, GMR appeared for 38 hours- annealed sample. Moreover, the sample annealed for 38 hours shows different GMR behavior at low temperatures compared with the sample annealed for 10 min., 1 hr. and 6 hrs.; GMR at low temperatures is smaller than those at high temperatures for the sample annealed for 38 hours. The magnetization curves at room temperature for the as-deposited and annealed samples show the superparamagnetic behavior. The magnetization curves is to be ferromagnetically below the blocking temperature. By analyzing the magnetization curves, we found that the magnetization behavior at low temperatures is to be more ferromagnetically with increasing annealing time. In case of sample annealed for 38 hours, the decrease of GMR at low temperatures seems to be related with the fact that the magnetization behavior at low temperatures is to be more ferromagnetically. We find that GMR is very sensitive to microstructure although the origin for the decrease in GMR is not definite at present.

Recently, we found that the enhancement of GMR at low temperatures in insulating granular systems can be interpreted by the effect of higher-order tunneling [17]. It is suggested that the change in GMR on annealing is related to the change of microstructure leading to the change of the contribution of higher-order tunneling compared with that of sequential tunneling.

4. Summary

We have investigated the change in GMR on annealing, in conjunction with the change in microstructure. The $Co_{46}Al_{19}O_{35}$ granular thin films were prepared on glass substrates by a reactive sputtering method with mixed gas of $Ar+O_2$. The samples were annealed at 300°C for 10 min., 1 hr., 6 hrs., 38 hrs. to change the microstructure. The magnitude of GMR decreases considerably with increasing annealing time, although the size of Co granules estimated from TEM observation show a small change. Parameter fits of magnetization curves to the Langevin function suggest that large clusters consisting of several small Co granules, which are coupled ferromagnetically, are related with the decrease of GMR on annealing. The temperature dependence of electrical resistivity (ρ) shows the relationship of log ρ versus $T^{-1/2}$ for the sample annealed for 10 min., 1 hr. and 6 hrs. However, the sample annealed for 38 hrs. shows the relationship of log ρ versus $T^{1/4}$, which represents a significant change in the transport mechanism. Although the transport mechanism was changed, GMR appeared for 38hours-annealed sample.

We find that GMR is very sensitive to microstructure.

Acknowledgments

I am very grateful to Dr. S. Mitani, Dr. K. Takanashi, Prof. H. Fujimori, Institute for Materials Research, Tohoku University, for their cooperation for the expriment and the usefull discussions. I also thanks to Dr. M. Ohnuma, Dr. K. Hono National Research Institute for Metals, for their cooperation for the TEM observation. This work was supported by a Grant-in-Aid for the Future Research from JSPS (Japan Society for the Promotion of Science), Japan, and for Scientific Research from Kwangwoon University, Korea, partially.

References

[1] M.N. Baibich, J.M. Broto, A. Fert, F. Nguyen Van Dau, F. Petroff, P. Eitenne, G. Creuzet, A. Friederich and J. Chazelas, Phys. Rev. Lett. 61, 2472 (1988).
[2] For a review, P.M. Levy, Solid State Phys. 47, 367 (1994).
[3] S. Zhang, P.M. Levy and A. Fert, Phys. Rev. B 45, 8689 (1992).
[4] J. Inoue and S. Maekawa, Phys. Rev. **B53**, 11927 (1996).
[5] H. Fujimori, S. Mitani and S. Ohnuma, Mater. Sci. Eng. **B31**, 219 (1995).
[6] S. Mitani, H. Fujimori and S. Ohnuma, J. Magn. Magn. Mater. **165**, 141 (1997).
[7] S. Maekawa and U. Gvert, IEEE Trans. Magn. **18**, 707 (1982).
[8] T. Miyazaki and N. Tezuka, J. Magn. Magn. Mater. **139**, L231 (1995).
[9] J. S. Moodera, L. R. Kinder, T. M. Wong and R. Meservey, Phys. Rev. Lett. **74**, 3273 (1995).
[10] Ping Sheng, B. Abeles and Y. Arie, Phys. Rev. Lett. **31**, 44 (1973).
[11] B. Abeles, Ping Sheng, M. D. Coutts and Y. Arie, Adv. Phys. **24**, 407 (1975).
[12] M. Ohnuma, K. Hono, E. Abe, H. Onodera, S. Mitani and H. Fujimori, J. Appl. Phys. **82**, 5646 (1997).
[13] N. F. Mott, Philos. Mag. **19**, 835 (1969).
[14] C. P. Bean, J. Appl. Phys. **26**, 1381 (1955).
[15] C. G. Granqvist and R. A. Buhrman, J. Appl. Phys. **47**, 2200 (1976).
[16] C. J. Adkins, Philos. Mag. **36**, 1285 (1977).
[17] S. Mitani, S. Takahashi, K. Takanashi, K. Yakushiji, S. Maekawa and H. Fujimori, Phys. Rev. Lett. **81**, 2799 (1998).